

# Discovery of very high energy $\gamma$ -rays associated with an X-ray binary

F. Aharonian<sup>1</sup>, A.G. Akhperjanian<sup>2</sup>, K.-M. Aye<sup>7</sup>, A.R. Bazer-Bachi<sup>3</sup>, M. Beilicke<sup>4</sup>,  
W. Benbow<sup>1</sup>, D. Berge<sup>1</sup>, P. Berghaus<sup>9</sup>, K. Bernlöhr<sup>1,5</sup>, C. Boisson<sup>6</sup>, O. Bolz<sup>1</sup>,  
V. Borrel<sup>3</sup>, I. Braun<sup>1</sup>, F. Breitling<sup>5</sup>, A.M. Brown<sup>7</sup>,  
J. Bussons Gordo<sup>12</sup>, P.M. Chadwick<sup>7</sup>, L.-M. Chounet<sup>8</sup>, R. Cornils<sup>4</sup>,  
L. Costamante<sup>1,20</sup>, B. Degrange<sup>8</sup>, H. J. Dickinson<sup>7</sup>, A. Djannati-Ataï<sup>9</sup>,  
L.O'C. Drury<sup>10</sup>, G. Dubus<sup>8\*</sup>, D. Emmanoulopoulos<sup>11</sup>, P. Espigat<sup>9</sup>, F. Feinstein<sup>12</sup>,  
P. Fleury<sup>8</sup>, G. Fontaine<sup>8</sup>, Y. Fuchs<sup>13</sup>, S. Funk<sup>1</sup>, Y.A. Gallant<sup>12</sup>, B. Giebels<sup>8</sup>,  
S. Gillessen<sup>1</sup>, J.F. Glicenstein<sup>14</sup>, P. Goret<sup>14</sup>, C. Hadjichristidis<sup>7</sup>,  
M. Hauser<sup>11</sup>, G. Heinzelmann<sup>4</sup>, G. Henri<sup>13</sup>, G. Hermann<sup>1</sup>,  
J.A. Hinton<sup>1</sup>, W. Hofmann<sup>1</sup>, M. Holleran<sup>15</sup>, D. Horns<sup>1</sup>,  
A. Jacholkowska<sup>12</sup>, O.C. de Jager<sup>15</sup>, B. Khélifi<sup>1</sup>, Nu. Komin<sup>5</sup>,  
A. Konopelko<sup>1,5</sup>, I.J. Latham<sup>7</sup>, R. Le Gallou<sup>7</sup>, A. Lemièrè<sup>9</sup>,  
M. Lemoine-Goumard<sup>8</sup>, N. Leroy<sup>8</sup>, T. Lohse<sup>5</sup>, A. Marcowith<sup>3</sup>,  
J.-M. Martin<sup>6</sup>, O. Martineau-Huynh<sup>16</sup>, C. Masterson<sup>1,20</sup>,  
T.J.L. McComb<sup>7</sup>, M. de Naurois<sup>16\*</sup>, S.J. Nolan<sup>7</sup>, A. Noutsos<sup>7</sup>,  
K.J. Orford<sup>7</sup>, J.L. Osborne<sup>7</sup>, M. Ouchrif<sup>16,20</sup>, M. Panter<sup>1</sup>,  
G. Pelletier<sup>13</sup>, S. Pita<sup>9</sup>, G. Pühlhofer<sup>1,11</sup>, M. Punch<sup>9</sup>, B.C. Raubenheimer<sup>15</sup>,  
M. Raue<sup>4</sup>, J. Raux<sup>16</sup>, S.M. Rayner<sup>7</sup>, A. Reimer<sup>17</sup>, O. Reimer<sup>17</sup>,  
J. Ripken<sup>4</sup>, L. Rob<sup>18</sup>, L. Rolland<sup>16</sup>, G. Rowell<sup>1</sup>,  
V. Sahakian<sup>2</sup>, L. Saugé<sup>13</sup>, S. Schlenker<sup>5</sup>, R. Schlickeiser<sup>17</sup>, C. Schuster<sup>17</sup>,  
U. Schwanke<sup>5</sup>, M. Siewert<sup>17</sup>, H. Sol<sup>6</sup>, D. Spangler<sup>7</sup>,  
R. Steenkamp<sup>19</sup>, C. Stegmann<sup>5</sup>, J.-P. Tavernet<sup>16</sup>, R. Terrier<sup>9</sup>,  
C.G. Théoret<sup>9</sup>, M. Tluczykont<sup>8,20</sup>, G. Vasileiadis<sup>12</sup>, C. Venter<sup>15</sup>,  
P. Vincent<sup>16</sup>, H.J. Völk<sup>1</sup>, S.J. Wagner<sup>11</sup>

\*To whom correspondence should be addressed; E-mail: denauroi@in2p3.fr, dubus@in2p3.fr

1. Max-Planck-Institut für Kernphysik, P.O. Box 103980, D 69029 Heidelberg, Germany
2. Yerevan Physics Institute, 2 Alikhanian Brothers St., 375036 Yerevan, Armenia
3. Centre d'Etude Spatiale des Rayonnements, CNRS/UPS, 9 av. du Colonel Roche, BP 4346, F-31029 Toulouse Cedex 4, France
4. Universität Hamburg, Institut für Experimentalphysik, Luruper Chaussee 149, D 22761 Hamburg, Germany
5. Institut für Physik, Humboldt-Universität zu Berlin, Newtonstr. 15, D 12489 Berlin, Germany
6. LUTH, UMR 8102 du CNRS, Observatoire de Paris, Section de Meudon, F-92195 Meudon Cedex, France
7. University of Durham, Department of Physics, South Road, Durham DH1 3LE, U.K.
8. Laboratoire Leprince-Ringuet, IN2P3/CNRS, Ecole Polytechnique, F-91128 Palaiseau, France
9. APC, UMR 7164 du CNRS, 11 Place Marcelin Berthelot, F-75231 Paris Cedex 05, France
10. Dublin Institute for Advanced Studies, 5 Merrion Square, Dublin 2, Ireland
11. Landessternwarte, Königstuhl, D 69117 Heidelberg, Germany
12. Laboratoire de Physique Théorique et Astroparticules, IN2P3/CNRS, Université Montpellier II, CC 70, Place Eugène Bataillon, F-34095 Montpellier Cedex 5, France
13. Laboratoire d'Astrophysique de Grenoble, INSU/CNRS, Université Joseph Fourier, BP 53, F-38041 Grenoble Cedex 9, France
14. DAPNIA/DSM/CEA, CE Saclay, F-91191 Gif-sur-Yvette, France
15. Unit for Space Physics, North-West University, Potchefstroom 2520, South Africa
16. Laboratoire de Physique Nucléaire et de Hautes Energies, IN2P3/CNRS, Universités Paris VI & VII, 4 Place Jussieu, F-75252 Paris Cedex 05, France
17. Institut für Theoretische Physik, Lehrstuhl IV: Weltraum und Astrophysik, Ruhr-Universität Bochum, D 44780 Bochum, Germany
18. Institute of Particle and Nuclear Physics, Charles University, V Holesovickach 2, 180 00 Prague 8, Czech Republic
19. University of Namibia, Private Bag 13301, Windhoek, Namibia
20. European Associated Laboratory for Gamma-Ray Astronomy, jointly supported by CNRS and MPG

**X-ray binaries are composed of a normal star in orbit around a neutron star or stellar-mass black hole. Radio and X-ray observations have led to the presumption that some X-ray binaries called microquasars behave as scaled down active galactic nuclei. Microquasars have resolved radio emission thought to arise from a relativistic outflow akin to active galactic nuclei jets, in which particles can be accelerated to large energies. Very high energy  $\gamma$ -rays produced by the interactions of these particles have been observed from several active galactic nuclei. Using the High Energy Stereoscopic System, we find the first evidence for gamma-ray emission  $>100$  GeV from a microquasar candidate, LS 5039, showing that particles are also accelerated to very high energies in these systems.**

High resolution radio maps of X-ray binaries (XRB) have revealed powerful outflows that are similar to the relativistic jets seen in active galactic nuclei (AGN) (1, 2). In both cases the radio emission is due to synchrotron radiation from particles accelerated to high energies. These outflows probably result from the accretion of material onto the compact object, albeit on vastly different scales: the mass (size) of black holes in AGN is at least  $10^6$  times larger than that of compact objects in XRB. Hence, XRB with resolved radio emission have been dubbed *microquasars*, reflecting the suspicion of some fundamental scaling with compact object mass.

The kinship should be most evident close to the black hole, where the jet is launched and where the available energy reservoir to accelerate particles is largest. In AGN the particles can reach energies such that their non-thermal emission extends to the GeV-TeV  $\gamma$ -ray regime via Compton upscattering of ambient photons or as a result of high energy hadron interactions. Because of relativistic bulk motion this emission is most easily seen in blazars, where the AGN jet is aligned close to the line-of-sight. Very high energy (VHE)  $\gamma$ -rays are to be expected from some XRB if the physical processes in the vicinity of the compact object are indeed analogous. However, previous observations of VHE emission from XRB remained inconclusive (3).

Two XRB have resolved milliarcsecond radio emission, which is presumed associated with a relativistic jet, and possible counterparts in the MeV-GeV domain (4–6). LS 5039 (RX J1826.2-1450) and LSI +61°303 (V615 Cas) are both composed of a massive star in an eccentric orbit around an undetermined compact object (7, 8). Their proposed  $\gamma$ -ray counterparts are respectively localised to  $0.5^\circ$  (3EG J1824-1514) and  $0.2^\circ$  (3EG J0241+6103) in the 3rd Energetic Gamma-Ray Experiment Telescope (EGRET) catalogue (9) so that the association cannot be considered firm on the basis of positional coincidence alone. The systems are quite inconspicuous in X-rays, with low variability and 1-10 keV luminosities  $\sim 10^{34}$  erg s $^{-1}$  (10, 11), which are about 10 times less than their luminosity above 100 MeV assuming that the EGRET sources are indeed counterparts. The  $\gamma$ -ray spectra measured by EGRET are hard with photon indexes  $\Gamma$  close to 2, suggesting emission could extend to the  $>100$  GeV regime where atmospheric Cherenkov Telescope (ACT) arrays operate. Constraining the emission cutoff energy provides important clues as to the physics of the  $\gamma$ -ray source. Furthermore, the XRB associations can be rigorously tested by the superior angular resolution of ACTs.

Located in the Southern Hemisphere, LS 5039 is ideally accessible to the High Energy Stereoscopic System (H.E.S.S.). H.E.S.S. is an ACT array of four telescopes located in Namibia, each equipped with a 107 m $^2$  mirror and a 960 photo-multiplier tube camera (12–14). The telescopes image the Cherenkov light from showers of particles created when VHE  $\gamma$ -rays and cosmic rays enter the atmosphere. A central trigger selects only showers seen by at least two telescopes. The combination of high resolution imaging and stereoscopic shower reconstruction allows efficient rejection of the background from cosmic ray initiated showers. The H.E.S.S.  $5\sigma$  sensitivity above 100 GeV reaches 1% of the Crab Nebula flux after 25 hours of observations close to the zenith. The direction of each  $\gamma$ -ray shower is determined to  $0.1^\circ$  accuracy, which enables arcmin localisation of sources within the  $5^\circ$  field-of-view.

The Galactic Plane survey carried out by the full H.E.S.S. array in the summer of 2004 testifies to the performance of the instrument. In (15) we reported on the discovery of eight *extended* VHE  $\gamma$ -ray sources within  $\pm 30^\circ$  of the Galactic Center and  $\pm 3^\circ$  of the Plane. After standard quality selection, a total of 25 pointings (10.5 h live time) taken during the scan were found to cover the position of LS 5039. The data were independently analysed with two separate calibration pipelines (16) and several different reconstruction methods, all of which were in excellent agreement with each other. The results presented here are based on a maximum likelihood adjustment of a shower model to the observed images to obtain the direction, impact parameter and energy of the primary (17). An image size cut of 60 photo-electrons was applied, corresponding to an average post-cut spectroscopic energy threshold of 220 GeV.

The reconstructed  $\gamma$ -ray map shows an excess  $1^\circ$  SW of the previously reported hotspot HESS J1825-137 (Fig. 1). The significance of the excess is calculated by comparing the number of source events, integrated over a circle of 6 arcmin, against the number of background events in several control regions located at the same distance to the camera center and excluding the nearby hotspot. We find a significance of more than  $7\sigma$  for this new source, denoted HESS J1826-148. The source is point-like with a size upper limit of  $50''$  ( $1\sigma$ ) given by a likelihood fit to a Gaussian source profile folded through the detector response. This is actually the only point like source discovered

in the Galactic scan (15). The best position is  $\alpha(\text{J2000})=18^{\text{h}}26^{\text{m}}15^{\text{s}}$  and  $\delta=-14^{\circ}49'30''$  with  $32''$  statistical and  $30''$  systematic uncertainties, which are comparable to that of the other survey sources (15). The positional accuracy is limited by the presence of an extended nearby source and systematics in observations taken at large offsets. On-axis observations are planned for 2005 and should improve the positional error to better than  $15''$ .

The  $\gamma$ -ray spectrum was derived from the comparison of reconstructed event energies to the prediction for a given spectral shape (18). The prediction uses energy resolutions and system acceptances derived from simulations, taking into account the zenith angle pointing of the array and the off-axis angle of the shower in the field-of-view for each observation. We find an acceptable fit ( $P(\chi^2) = 7\%$ ) to a power-law with a photon index  $\Gamma = 2.12 \pm 0.15$  (Fig. 2). The low statistics currently limit further investigation of more complex spectral shapes. The average integral flux above 250 GeV is  $5.1 \pm 0.8_{\text{stat}} \pm 1.3_{\text{syst}} \times 10^{-12}$  ph cm $^{-2}$  s $^{-1}$ , corresponding to a luminosity  $\approx 10^{33}$  erg s $^{-1}$  at 3 kpc (11). Errors on the spectral parameters correspond to  $1\sigma$  confidence interval. The highest energy measurement is at  $\approx 4$  TeV.

The positions of the supernova remnant G016.8-01.1 and pulsar PSR B1822-14, which are both in the error box of the EGRET source and plausible  $\gamma$ -ray sources, are inconsistent with the position of HESS J1826-148 (Fig. 1). Production of  $\gamma$ -rays from the interaction of cosmic-rays with the interstellar medium is precluded by the low H column density at the location of HESS J1826-148 compared to its surroundings (19). The radio position of LS 5039 is  $84''$  away from the H.E.S.S. position and well within the  $3\sigma$  confidence region (Fig. 1). We checked there are no other radio or X-ray sources compatible with HESS J1826-148 in the NRAO VLA 1.4 GHz Sky Survey (20) and in the XMM/Chandra fields analysed by (21). The observations are not simultaneous with those of H.E.S.S. so we cannot formally exclude a long episode of flaring from a blazar. That this blazar is not detected in radio would be surprising as their emission at this wavelength is persistent at levels  $\geq 100$  mJy well above the survey sensitivity (3 mJy for a point source). The present evidence largely favours the association of LS 5039 with HESS J1826-148 and, by extrapolation, with the unidentified EGRET source 3EG 1824-1514. The present H.E.S.S. data is consistent with a constant flux (Fig. S1). Confirmed  $\gamma$ -ray variability correlated with other wavebands or a telltale modulation would fully establish the association.

Several processes can lead to  $\gamma$ -ray emission in LS 5039. The bulk of the luminosity in the system is emitted by the O6.5V stellar companion ( $L_* \approx 10^{39}$  erg s $^{-1}$ ) at an energy  $kT_* \approx 3.5$  eV (Fig. 2). The binary separation varies from  $2R_*$  to  $6R_*$  ( $R_* \approx 7 \cdot 10^{11}$  cm), and the radiation density reaches  $n_* \approx 10^{14}$  photons cm $^{-3}$  close to the compact object. These stellar photons can be boosted to  $\gamma$ -ray energies by inverse Compton scattering on VHE electrons (22). With such radiation densities the energy loss timescale for electrons in the deep Klein-Nishina regime, giving a strict upper limit on the radiative timescale, is  $\sim 300$  s. A short radiative timescale compared to the escape timescale from the system ( $\sim 100$  s) implies that inverse Compton emission can be very efficient.

Accelerating electrons to the required energies may be hindered by such rapid losses. Very high energies may be easier to reach for protons, which suffer fewer radiation losses. VHE  $\gamma$ -rays may then be emitted via  $pp$  interactions with the stellar wind. Assuming a stellar wind with a mass loss rate of  $10^{-6} M_{\odot}$  yr $^{-1}$  and velocity 1000 km s $^{-1}$ , the density at  $2R_*$  is  $\sim 10^{10}$  protons cm $^{-3}$ . For such a density the  $pp$  interaction timescale is  $\sim 10^5$  s. At least  $10^2/10^5=0.1\%$  of the protons radiate for free streaming particles, implying a total kinetic energy less than  $10^{38}$  erg s $^{-1}$ . Protons may also interact with stellar photons but the threshold is very high  $\sim 10^{17}$  eV. The  $p\gamma$  timescale is  $\sim 10^3$  s.

Photons emitted in the H.E.S.S. energy range can interact with the 3.5 eV stellar radiation before leaving the system, producing  $e^+e^-$  pairs. The cross-section maximum  $\sigma_{\gamma\gamma} \approx 1.7 \cdot 10^{-25}$  cm $^2$  occurs for  $\gamma$ -rays of energy  $\approx 100$  GeV. The opacity is  $\tau_{\gamma\gamma} = \sigma_{\gamma\gamma} n_* r \approx 20$  for a photon travelling a distance  $r \approx 10^{12}$  cm comparable to the binary separation. VHE photons emitted close to the compact object are therefore always well inside the ‘ $\gamma$ -photosphere’ at which  $\tau_{\gamma\gamma} \approx 1$ . This initiates an  $e^+e^-$  pair cascade that redistributes the absorbed radiation to lower frequencies. Gamma-rays at energies below 100 GeV suffer little absorption because of the Wien cutoff of the stellar spectrum. At higher energies the opacity decreases as  $1/E_{\gamma}$  (23). The VHE spectrum may therefore be hardened compared to its intrinsic shape.

The absorption of TeV photons in the system can be mitigated. First, the cross-section threshold and amplitude are angle-dependent so that  $\gamma$ -rays emitted in a cone pointing away from the companion are not absorbed.

Scattering of stellar photons in the wind will tend to isotropize the radiation and diminish this effect. Variations are expected since the geometry changes with orbital phase. Second,  $\gamma$ -ray emission need not take place close to the compact object. Observations of X-ray emission from XRB jets provides evidence for acceleration of electrons to TeV energies on parsec scales (24). In LS 5039, acceleration at a shock  $>1$  AU away from the stellar companion would happen beyond the  $\gamma$ -photosphere.

The association of LS 5039 with HESS J1826-148 confirms that like some AGN, XRB are able to accelerate particles to at least TeV energies. Shocks from colliding ejecta or from jet - interstellar medium interactions are natural candidates. Yet the association with an outflow may be questioned in the absence of a direct detection of relativistic motion in radio. The relativistic wind of a young pulsar is a conceivable alternative for particle injection (25). The situation would then resemble that in PSR B1259-63, a system composed of a radio pulsar in a much wider 3.4 yr eccentric orbit around a Be star. TeV emission from PSR B1259-63 was detected with H.E.S.S. close to periastron (26). The higher wind density in LS 5039 probably smears out any radio pulses. The resolved radio emission from LS 5039 would be due to particles (cascade pairs) streaming out of the system. Further insights into this system may be gained from combined radio and  $\gamma$ -ray observations: Very Long Baseline Array maps attain a spatial resolution of a few AU (6) tantalizingly close to the  $\gamma$ -photosphere.

## References and Notes

1. I. F. Mirabel, L. F. Rodriguez, *Nature* **371**, 46 (1994).
2. A. P. Marscher, *et al.*, *Nature* **417**, 625 (2002).
3. T. C. Weekes, *Space Science Reviews* **59**, 315 (1992).
4. P. C. Gregory, A. R. Taylor, *Nature* **272**, 704 (1978).
5. A. R. Taylor, H. T. Kenny, R. E. Spencer, A. Tzioumis, *Astrophys. J.* **395**, 268 (1992).
6. J. M. Paredes, J. Martí, M. Ribó, M. Massi, *Science* **288**, 2340 (2000).
7. J. B. Hutchings, D. Crampton, *Publ. Astronom. Soc. Pacific* **93**, 486 (1981).
8. M. V. McSwain, *et al.*, *Astrophys. J.* **600**, 927 (2004).
9. R. C. Hartman, *et al.*, *Astrophys. J. Suppl. Ser.* **123**, 79 (1999).
10. G. F. Bignami, P. A. Caraveo, R. C. Lamb, T. H. Markert, J. A. Paul, *Astrophys. J.* **247**, L85 (1981).
11. C. Motch, F. Haberl, K. Dennerl, M. Pakull, E. Janot-Pacheco, *Astron. Astrophys.* **323**, 853 (1997).
12. K. Bernlöhner, *et al.*, *Astroparticle Physics* **20**, 111 (2003).
13. J. A. Hinton, *New Astronomy Review* **48**, 331 (2004).
14. S. Funk, *et al.*, *Astroparticle Physics* **22**, 285 (2004).
15. F. Aharonian, *et al.*, *Science* **307**, 1938 (2005).
16. F. Aharonian, *et al.*, *Astroparticle Physics* **22**, 109 (2004).
17. M. de Naurois, *et al.*, *Proc. of the 28<sup>th</sup> ICRC (Tsukuba)* (2003), p. 2907.
18. F. Piron, *et al.*, *A&A* **374**, 895 (2001).
19. M. Ribó, *et al.*, *Astron. Astrophys.* **384**, 954 (2002).
20. J. J. Condon, *et al.*, *Astronomical Journal* **115**, 1693 (1998).
21. A. Martocchia, C. Motch, I. Negueruela, *Astron. Astrophys.* **430**, 245 (2005).

22. V. Bosch-Ramon, J. M. Paredes, *Astron. Astrophys.* **417**, 1075 (2004).
23. R. J. Gould, G. P. Schröder, *Phys. Rev.* **155**, 1408 (1967).
24. S. Corbel, *et al.*, *Science* **298**, 196 (2002).
25. L. Maraschi, A. Treves, *Mon. Not. R. Astron. Soc.* **194**, 1P (1981).
26. M. Beilicke, M. Ouchrif, G. Rowell, S. Schlenker, *IAUC* **8300**, 2 (2004).
27. N. J. Tasker, J. J. Condon, A. E. Wright, M. R. Griffith, *Astronom. J.* **107**, 2115 (1994).
28. M. Ribó, P. Reig, J. Martí, J. M. Paredes, *Astron. Astrophys.* **347**, 518 (1999).
29. J. Martí, J. M. Paredes, M. Ribo, *Astron. Astrophys.* **338**, L71 (1998).
30. J. S. Clark, *et al.*, *Astron. Astrophys.* **376**, 476 (2001).
31. The support of the Namibian authorities and of the University of Namibia in facilitating the construction and operation of H.E.S.S. is gratefully acknowledged, as is the support by the German Ministry for Education and Research (BMBF), the Max Planck Society, the French Ministry for Research, the CNRS-IN2P3 and the Astroparticle Interdisciplinary Programme of the CNRS, the U.K. Particle Physics and Astronomy Research Council (PPARC), the IPNP of the Charles University, the South African Department of Science and Technology and National Research Foundation, and by the University of Namibia. We appreciate the excellent work of the technical support staff in Berlin, Durham, Hamburg, Heidelberg, Palaiseau, Paris, Saclay, and in Namibia in the construction and operation of the equipment.

**Supporting Online Material:** Fig. S1

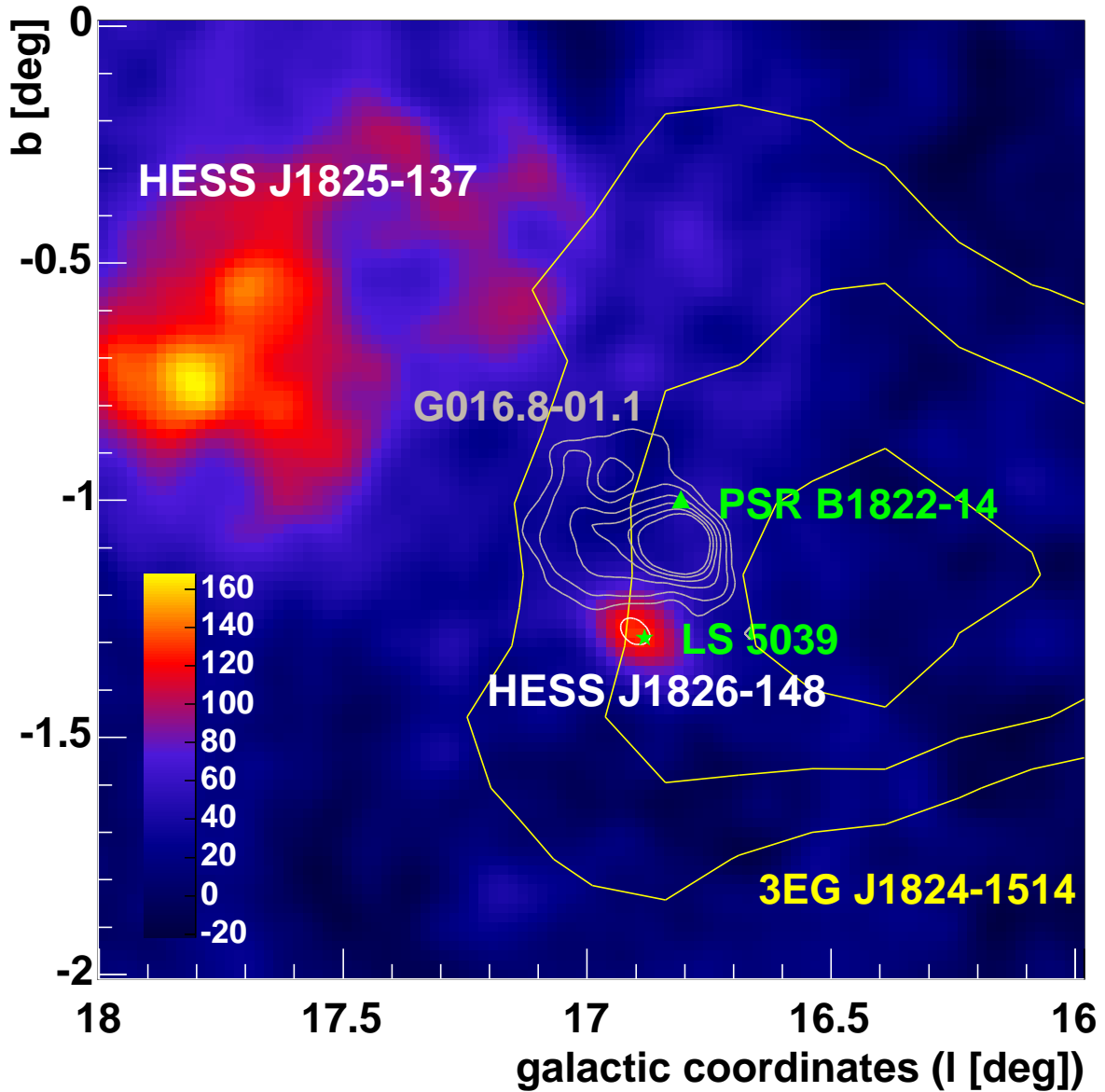


Figure 1: Map of excess  $\gamma$ -ray emission in units of counts for the region around LS 5039. The map has been smoothed by the point spread function. The white ellipse shows the  $3\sigma$  confidence region for HESS J1826-148. The radio emission from the SNR G016.8-01.1 is represented by gray contours (0.05, 0.1, 0.2, 0.3, 0.4 and 0.5 Jy/beam) obtained from the Parkes-MIT-NRAO 6 cm radio survey map (27, 28). The yellow contours show the 68%, 95% and 99% confidence level region of the EGRET source 3EG J1824-1514. The green star marks the position of the radio source associated with the microquasar LS 5039. HESS J1825-137 is discussed in (15).

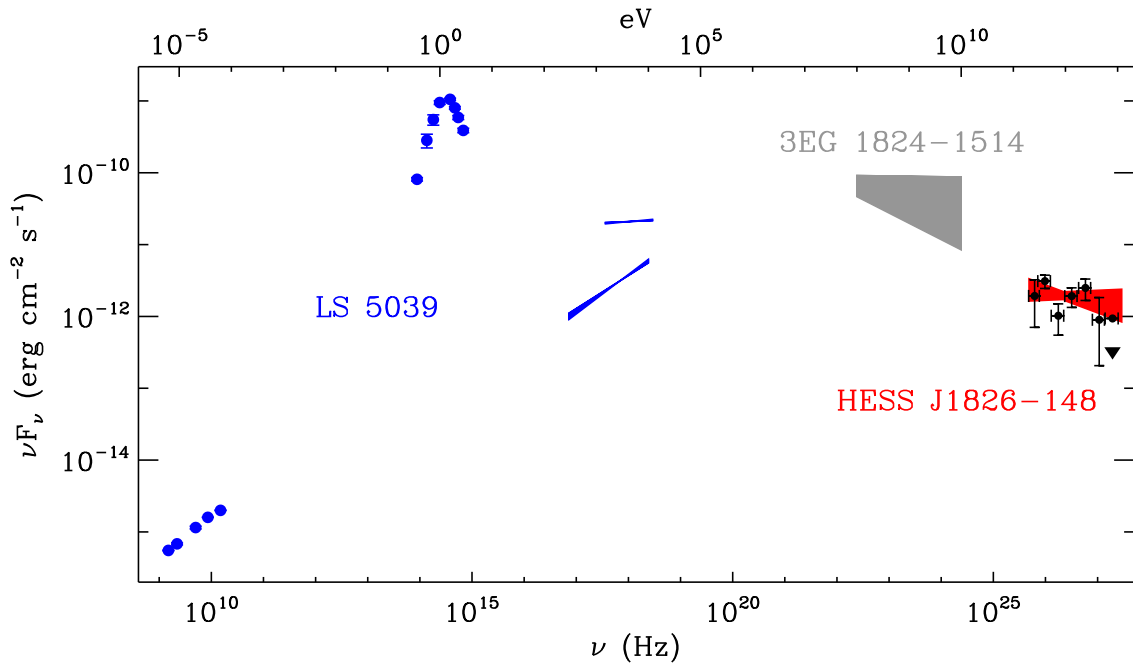


Figure 2: Spectral Energy Distribution of LS 5039 including the spectrum of HESS J1826-148 (points in black, power law fit in red). The average radio, IR, optical and X-ray fluxes are shown in blue (21, 28–30). Optical fluxes are not dereddened. The two X-ray spectra correspond to the historical 1998 high (Rossi X-ray Timing Explorer, RXTE) and 2003 low (X-ray Multi-mirror Mission, XMM) flux observations of LS 5039. The multi-year average flux above 100 MeV from the EGRET source 3EG J1824-1514 is shown in grey (9).



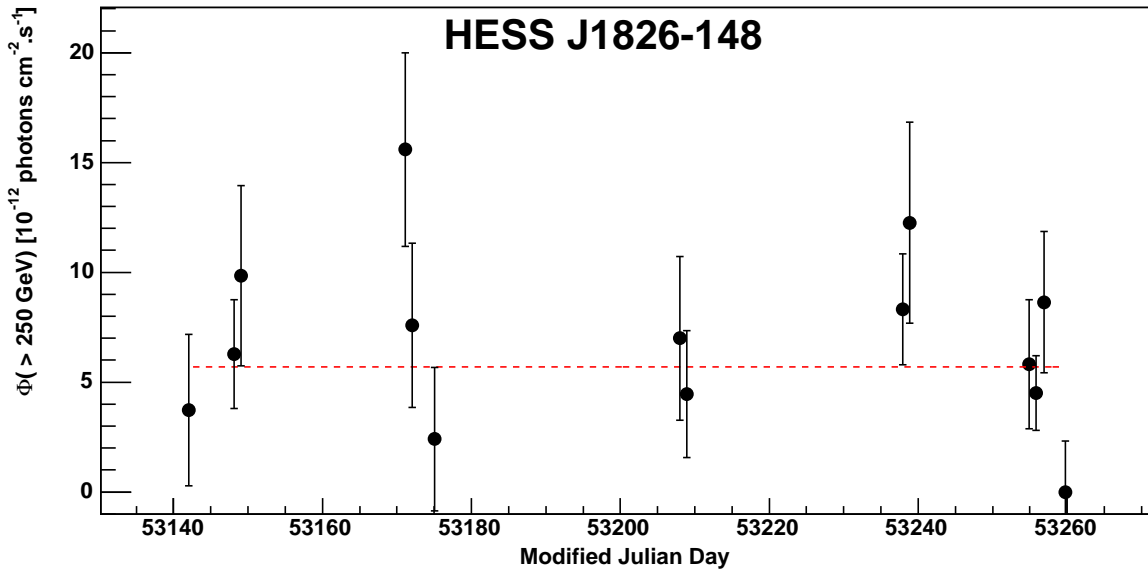


Figure 3: ONLINE MATERIAL. Night by night integral flux above 250 GeV of HESS J1826-148. Taking into account a 20% systematic uncertainty, the hypothesis of a constant flux over the four months time span is acceptable at the 15% confidence level. The H.E.S.S. data covers  $\sim 27$  cycles of the 4.4 day orbital period roughly uniformly in phase. No periodic variations are apparent when folding the data using the orbital ephemeris of (8). The highest peak in a 2-100 day Lomb-Scargle periodogram of the run by run fluxes has a significance  $< 2 \sigma$ . The statistics are insufficient to study daily variations in the spectral parameters.